applied optics

High precision automated alignment procedure for two-mirror telescopes

Karen M. Hampson,[1,*] David Gooding,[2] Robin Cole,[2] and Martin J. Booth[1]

[1]Department of Engineering Science, University of Oxford, 17 Parks Rd., Oxford OX1 3PJ, UK
[2]Surrey Satellite Technology Ltd., Surrey Research Park, Guildford GU2 7YE, UK
*Corresponding author: karen.hampson@eng.ox.ac.uk

Received 24 April 2019; revised 17 July 2019; accepted 25 July 2019; posted 29 July 2019 (Doc. ID 365913); published 12 September 2019

A significant challenge in the production of Earth observation satellites is the precise alignment of the telescope optical components. We have developed a strategy to perform automated alignment of two-mirror telescopes for use in a realistic factory-based setting. A Ritchey–Chrétien telescope was used as an example. The secondary mirror was mounted on a high precision hexapod and its misalignment inferred from the Zernike coefficients for tilt, defocus, and coma, as measured by a phase-shifting interferometer. The required corrections to the position of the secondary mirror were implemented using an integral controller and alignment was achieved within minutes, compared to within days when using a manual alignment process. The Zernike coefficient for each aberration was reduced to within one standard deviation of the fluctuations due to residual instability (48 nm).

https://doi.org/10.1364/AO.58.007388

1. INTRODUCTION

A misaligned telescope can lead to aberrated images and is a major cause of failure of satellite missions with optical imaging payloads. A typical industrial approach to aligning the telescope optics during the build phase is manual. For example, in alignment of a two-mirror telescope, such as a Ritchey–Chrétien telescope, the secondary mirror is aligned to the primary mirror in a double-pass configuration, using adjustments informed by observation of the point spread function of an alignment laser, or from live interferometry. These are heuristic and time-consuming techniques that can have a significant impact on build schedule.

A number of procedures have been examined to assist in the alignment of telescopes [1–13]. Arguably, the most widely used quantitative methods are based upon determining the sensitivity of Zernike coefficients or Seidel coefficients to the movement of the secondary mirror [5,8–12]. This is typically carried out using an optical model of the system. Using this data, the necessary movements of the mirror are determined based on real measurements from the misaligned system. However, results from optical models may not necessarily translate into practice [5]. Aberrations introduced with each degree of freedom are coupled and there is a non-linear relationship between these aberrations and the magnitude of the misalignment. Furthermore, some studies use measurements of aberrations or image quality on-axis and at several off-axis positions, making the alignment process more arduous [1,2]. However, by including considerations of pointing errors, which manifest as tip and tilt, only on-axis measurements are required [3,5]. Here we present and demonstrate a simple fully automated alignment algorithm for a two-mirror telescope using a Ritchey–Chrétien telescope as an example. Alignment is achieved within 3 to 4 min using only on-axis measurement of aberrations and no optical modeling is required.

2. OPTICAL SETUP

The optical setup is shown in Fig. 1. Light from a fiber-coupled frequency stabilized 5 mW HeNe laser (SL_02, SIOS) was coupled into a phase-shifting interferometer (μPhase 1000, Trioptics). The light leaving the interferometer was focused at the focus of the telescope and was reflected from the secondary mirror (custom made, Oldham Optical UK) onto the primary mirror (custom made, Oldham Optical UK). The specifications of these mirrors are shown in Table 1. The light was then reflected from a flat mirror (custom made, Optical Surfaces Ltd.) and passed back through the telescope to the interferometer. The secondary mirror was attached to a hexapod (HXP50-MECA, Newport), which has a precision of 0.1 μm or less for translational movements and 0.1 mdeg or less for rotational movements. The hexapod had a range of ±7 mm in z, ±15 mm in x and y, ±9° in θx, ±8.5° in θy, and ±18° in θz. The frame of the telescope tower consisted of aluminum columns. The breadboard (B7575L, Thorlabs) was mounted on passive isolation mounts (PWA075, Thorlabs) to

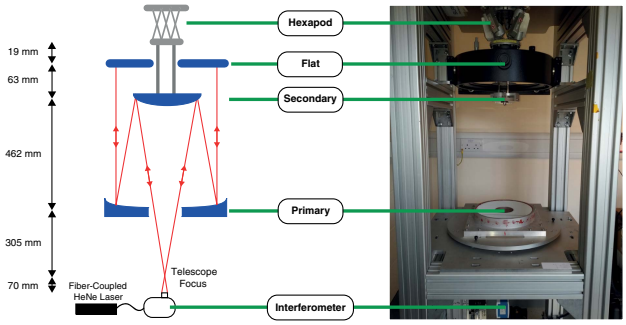

Fig. 1. Telescope construction showing the primary mirror, secondary mirror, flat mirror, hexapod, and interferometer.

Table 1. Primary and Secondary Mirror Parameters

Mirror	Focal Length (mm)	Diameter (mm)	Conic
Primary	745	250	−1.23
Secondary	448.5	100	−7.07

reduce vibrations. The telescope construction mimicked that used by Surrey Satellite Technology Ltd. during the build phase of their telescopes.

3. ALIGNMENT PROCEDURE

A correctly aligned Ritchey–Chrétien telescope has no intrinsic coma. Coma is the most significant aberration introduced when the secondary mirror in a Ritchey–Chrétien telescope is either displaced perpendicular to the optical axis (decenter), or rotated about its vertex [3,14,15]. Consequently, the magnitude of coma is a good criterion for determining misalignment. As coma introduced by decenter can be offset by that introduced by tilting the mirror, zero coma does not guarantee that the two mirrors are aligned [14]. Hence pointing errors, which manifest as tip and tilt, are of value to inform alignment. Despace (translation along the optical axis) determines the amount of defocus present [14]. However, when the axis of the secondary mirror is not concurrent with that of the primary, other modes aside from defocus are introduced.

A flow chart outlining the procedure for automated alignment of the secondary mirror, along with example results, is shown in Fig. 2. The algorithm was implemented in Python. Zernike coefficients were obtained from the interferometer using the μPhase commercial software (Trioptics). The code will be freely available from the authors on request. The coefficients used for the alignment were vertical tilt, c_{vTilt}; horizontal tilt, c_{hTilt}; defocus, c_{Def}; vertical coma, c_{vComa}; and horizontal coma, c_{hComa}.

Vertical and horizontal tilt were first corrected via decentration (Dec) and rotation of the secondary mirror about its vertex (Rot). Owing to non-linearities in the relationship between the Zernike coefficients and movement of the mirror, the required correction was implemented using an integral controller [16]:

$$\begin{bmatrix} \mathrm{Dec}_x \\ \mathrm{Dec}_y \\ \mathrm{Rot}_x \\ \mathrm{Rot}_y \end{bmatrix}_{i+1} = \begin{bmatrix} \mathrm{Dec}_x \\ \mathrm{Dec}_y \\ \mathrm{Rot}_x \\ \mathrm{Rot}_y \end{bmatrix}_{i} - g \times \begin{bmatrix} s_{Dx,\mathrm{vTilt}} & s_{Dx,\mathrm{hTilt}} \\ s_{Dy,\mathrm{vTilt}} & s_{Dy,\mathrm{hTilt}} \\ s_{Rx,\mathrm{vTilt}} & s_{Rx,\mathrm{hTilt}} \\ s_{Ry,\mathrm{vTilt}} & s_{Ry,\mathrm{hTilt}} \end{bmatrix} \begin{bmatrix} c_{\mathrm{vTilt}} \\ c_{\mathrm{hTilt}} \end{bmatrix}_{i+1}, \tag{1}$$

where i is the iteration number, g is the gain, and s are the sensitivities of each Zernike coefficient to movements of the telescope. For example, $s_{Dx,\mathrm{vTilt}}$ represents the sensitivity of vertical tilt to a decentration in the x direction. The sensitivities were determined using

$$s_{(\mathrm{Move,Zern})} = \frac{Z^{+} - Z^{-}}{\mathrm{Move}^{+} - \mathrm{Move}^{-}}, \tag{2}$$

where Z^{+} is the Zernike coefficient when moving the secondary mirror in the positive direction by an amount Move^{+}, and Z^{-} is the Zernike coefficient when moving the secondary mirror in the negative direction by an amount Move^{-}. Table 2 shows the values for the movements and sensitivities. The movements were chosen such that the interferometer signal was not vignetted. A gain of 0.8 was used and Eq. (1) is repeated until c_{vTilt} and c_{hTilt} fall below a given threshold, $\mathrm{Tilt}_{\mathrm{Thres}}$. Owing to residual instabilities in the system due to vibrations, the threshold was chosen as the mean of the standard deviations of each Zernike coefficient measured 100 times. This value was 48 nm and was used as the threshold for all Zernike coefficients. These fluctuations can be reduced by using active vibration isolation rather than passive vibration isolation.

Once vertical and horizontal tilt are corrected, the Zernike coefficients are measured again. If the amount of defocus is above the threshold $\mathrm{Def}_{\mathrm{Thres}}$, then defocus is corrected via

$$\mathrm{Des}_{i+1} = \mathrm{Des}_i - g \times s_{\mathrm{Des,Def}} \times c_{\mathrm{Def}i+1}, \tag{3}$$

where Des is the despace position of the mirror. A gain of one was used. Once corrected, the coefficients are again measured, and if any of the coma coefficients are above the threshold, coma is corrected by rotating the mirror about its center of curvature (RCOC) using

$$\mathrm{RCOC}_{xi+1} = R_{v\mathrm{Coma}i} - g \times s_{x\mathrm{Coma}} \times c_{v\mathrm{Coma}i+1}, \tag{4}$$

$$\mathrm{RCOC}_{yi+1} = R_{h\mathrm{Coma}i} - g \times s_{y\mathrm{Coma}} \times c_{h\mathrm{Coma}i+1}. \tag{5}$$

Again, a gain of one was used. Rotation of the mirror results in intersection of the axis of the secondary mirror with that of the primary [14]. The rotation need not be around the center of curvature.

Finally, the Zernike coefficients are measured again, and the cycle is repeated until all coefficients fall below the given threshold. Each measurement of the Zernike coefficients and adjustment of the secondary mirror takes around 6 s. Typically, four to five loops of the algorithm are required to complete the alignment algorithm and alignment is achieved within 3 to 4 min. Figure 2(b) shows an example of the time evolution of each Zernike coefficient during the correction procedure for two different starting misalignments, (i) and (ii). The x axis represents the n umber of measurements of Zernike aberrations and adjustments of the mirror position. Repeated measurement

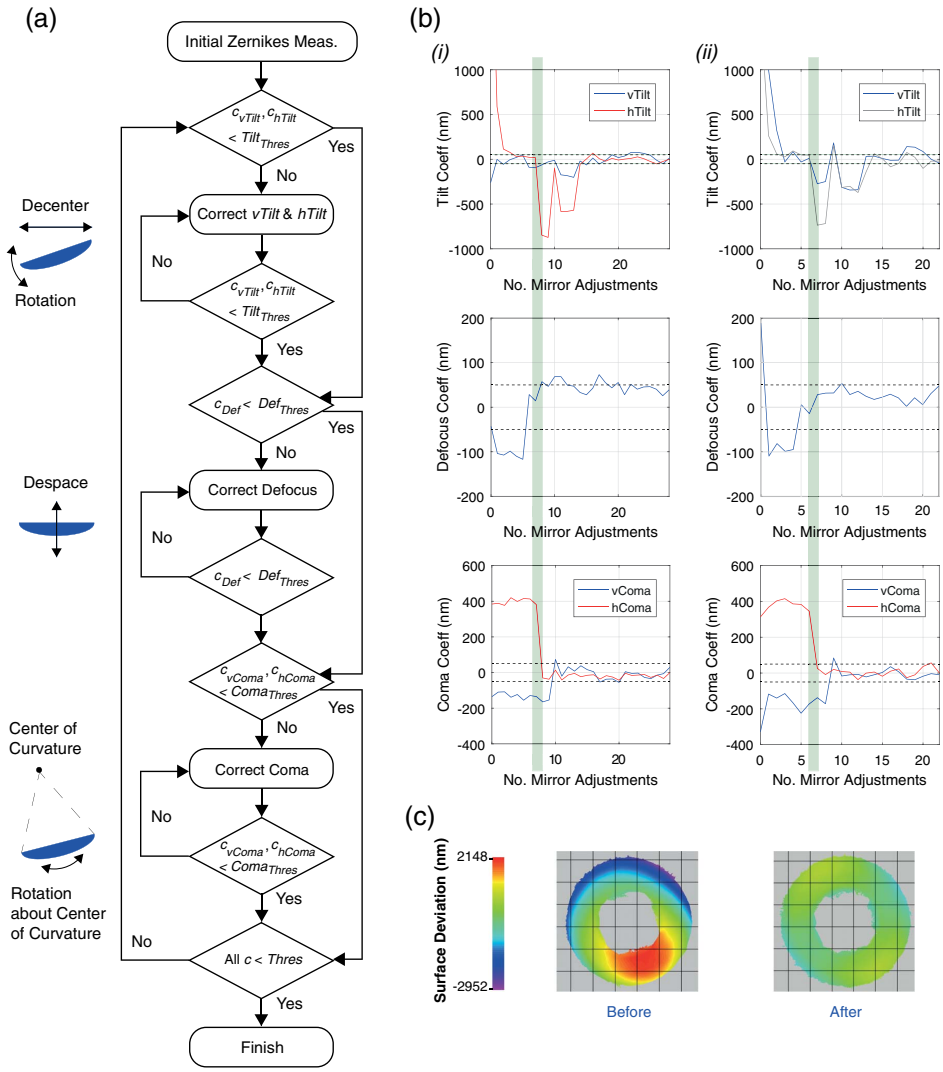

Fig. 2. (a) Procedure for automated alignment. (b) Example data from two different misalignments. Shaded regions show the coupling between horizontal coma and horizontal tilt. When horizontal coma was corrected, horizontal tilt became more negative. (c) Example wavefront map before and after correction.

Table 2. Sensitivity of the Zernike Coefficients to Movements of the Secondary Mirror[a]

Movement	Movement Value	Sensitivity
Dec_x	±0.04 mm	$S_{Dx,\mathrm{vTilt}} = 1.2 \times 10^5$ nm/mm $S_{Dx,\mathrm{hTilt}} = -66$ nm/mm
Dec_y	±0.04 mm	$S_{Dx,\mathrm{vTilt}} = 26$ nm/mm $S_{Dx,\mathrm{hTilt}} = -1.2 \times 10^5$ nm/mm
Rot_x	±0.002 deg	$S_{Rx,\mathrm{vTilt}} = -1.5 \times 10^4$ nm/deg $S_{Rx,\mathrm{hTilt}} = -1.9 \times 10^6$ nm/deg
Rot_y	±0.002 deg	$S_{Rx,\mathrm{vTilt}} = -1.9 \times 10^6$ nm/deg $S_{Rx,\mathrm{hTilt}} = -9 \times 10^3$ nm/deg
Des	±0.05 mm	$S_{\mathrm{Des,vTilt}} = -1.5 \times 10^{-5}$ nm/mm
$RCOC_x$	±0.01 deg	$S_{\mathrm{SCOCR},v\mathrm{comma}} = -2.7 \times 10^{-6}$ nm/deg
$RCOC_y$	±0.01 deg	$S_{\mathrm{SCOCR},h\mathrm{comma}} = -3.8 \times 10^{-6}$ nm/deg

[a]The movements are decenter (Dec), in the x and y directions; rotation (Rot) of the mirror about its vertex, in the x and y directions; despacing (Des); and rotation about the center of curvature (RCOC), in the x and y directions.

of the Zernike coefficients at each stage is necessary owing to the coupling between the coefficients. When correcting for horizontal coma, for example, by rotating the secondary mirror about its center of curvature, horizontal tilt is also affected. This coupling is highlighted in the shaded regions of the graphs. The initial and final rms wavefront error, across the five coefficients manipulated during the alignment process, was (3.3×10^3 nm, 0.05×10^3 nm) for the first example and (5.8×10^3 nm, 0.07×10^3 nm) for the second example. Figure 2(c) shows an example of a wavefront map before and after correction. The residual astigmatism in the wavefront map was found to be due to astigmatism in the primary mirror. Modeling using Zemax confirmed the relationship between misalignments of the secondary mirror and changes in the Zernike aberration coefficients.

This algorithm is directly applicable to other two-mirror telescopes. Although other two-mirror telescopes, such as the classic Cassegrain telescope, are not intrinsically free of coma,

when the telescope is aligned correctly, there is no coma on axis. Consequently, elimination of coma, pointing errors, and defocus, at the center of the field, will yield the correct placement of the secondary mirror [3].

4. CONCLUSION

We have demonstrated an automated alignment procedure for the secondary mirror of two-mirror telescopes using a hexapod to adjust the mirror position based on feedback from an interferometer. Non-linearities in the change in the Zernike coefficients with movement of the mirror were circumvented by implementing correction via an integral controller. Repeated sequential correction of Zernike coefficients was sufficient to overcome coupling. This approach rapidly speeds up the alignment compared to manual alignment, and allows inherent quantification of alignment quality to compare with requirements and improve consistency within batch builds. Future work will include the development of an alignment strategy that uses live Earth images to inform in-orbit alignment [17].

Funding. Centre for Earth Observation Instrumentation (EO10-PF-019); Engineering and Physical Sciences Research Council (EP/R511742/1).

REFERENCES

1. J. W. Figoski, T. E. Shrode, and G. F. Moore, "Computer-aided alignment of a wide-field, three-mirror, unobscured, high-resolution sensor," Proc. SPIE **1049**, 166–177 (1989).
2. B. A. McLeod, "Collimation of fast wide-field telescopes," Publ. Astron. Soc. Pac. **108**, 217–219 (1996).
3. D. R. Blanco, "Near-perfect collimation of wide-field Cassegrain telescopes," Publ. Astron. Soc. Pac. **124**, 36–41 (2012).
4. J. Lim, S. Lee, I. K. Moon, H.-S. Yang, J. U. Lee, Y.-J. Choi, J.-H. Park, and H. Jin, "Sensitivity analysis of a wide-field telescope," J. Korean Phys. Soc. **63**, 28–35 (2013).
5. E. Oh, K.-B. Ahn, and S.-W. Kim, "Experimental sensitivity table method for precision alignment of Amon-Ra instrument," J. Astron. Space Sci. **31**, 241–246 (2014).
6. C. Pernechele, F. Bortoletto, and K. Reif, "Hexapod control for an active secondary mirror: general concept and test results," Appl. Opt. **37**, 6816–6821 (1998).
7. E. Luna, A. Cordero, J. Valdez, L. Gutiérrez, and L. Salas, "Telescope alignment by out-of-focus stellar image analysis," Publ. Astron. Soc. Pac. **111**, 104–110 (1999).
8. E. Luna, S. Zazueta, and L. Gutiérrez, "An innovative method for the alignment of astronomical telescopes," Publ. Astron. Soc. Pac. **113**, 379–384 (2001).
9. S. Kim, H.-S. Yang, Y.-W. Lee, and S.-W. Kim, "Merit function regression method for efficient alignment control of two-mirror optical systems," Opt. Express **15**, 5059–5068 (2007).
10. A. M. Manuel and J. H. Burge, "Alignment aberrations of the new solar telescope," Proc. SPIE **7433**, 74330A (2009).
11. E. D. Kim, Y.-W. Choi, M.-S. Kang, and S. C. Choi, "Reverse-optimization alignment algorithm using Zernike sensitivity," J. Opt. Soc. Korea **9**, 68–73 (2005).
12. W. Bin, J. S. Lei, and Q. Tian, "Study on computer-aided alignment method of Cassegrain system," Proc. SPIE **7654**, 765405 (2010).
13. E. E. Bloemhof, X. An, G. Kuan, D. Moore, B. O'Shay, N. Page, and H. Tang, "Telescope alignment from sparsely sampled wavefront measurements over pupil subapertures," Appl. Opt. **51**, 394–400 (2012).
14. V. N. Mahajan, "Calculation of primary aberrations: perturbed optical systems," in *Optical Imaging and Aberrations: Part 1. Ray Geometrical Optics* (SPIE, 1998), pp. 435–460.
15. W. B. Wetherell and M. P. Rimmer, "General analysis of aplanatic Cassegrain, Gregorian, and Schwarzschild telescopes," Appl. Opt. **11**, 2817–2832 (1972).
16. K. M. Hampson, "Adaptive optics and vision," J. Mod. Opt. **55**, 3425–3467 (2008).
17. D. Gooding, G. Richardson, A. Haslehurst, D. Smith, C. Saunders, G. Aglietti, R. Blows, J. Shore, K. M. Hampson, and M. Booth, "A novel deployable telescope to facilitate a low-cost <1m GSD video rapid-revisit small satellite constellation," in *Proceedings of the International Conference on Space Optics* (2019).